INTRINSIC INHOMOGENEITIES IN ANTIFERROMAGNETS AND SUPERCONDUCTORS

V.V. EREMENKO, V.A. SIRENKO

Institute for Low Temperature Physics and Engineering, Nat. Acad. Sci. of Ukraine
(47, Lenin Ave., Kharkiv 61103, Ukraine; E-mail: eremenko@ilt.kharkov.ua)

UDC 535.343.2

The common features of the formation of inhomogeneous magnetic states in uniaxial antiferromagnets and superconductors in the vicinity of phase transitions induced by an external magnetic field are considered. The experimental data on the transverse magnetization component are analyzed for the uniaxial crystals of superconducting dichalcogenide 2H-$NbSe_2$ and antiferromagnetic ferrous carbonate $FeCO_3$ in the framework of thermodynamic approach.

1. Introduction

This article considers similarities in the formation of intrinsic magnetic states in antiferromagnets and superconductors. Recently, the inhomogeneous ground state gained in a paramount importance due to thorough investigation of the advantageous properties of manganites and nanosized objects. Apparently [1], the ground states of manganite models tend to be intrinsically inhomogeneous because of strong tendencies toward phase separation, typically involving ferromagnetic metallic and antiferromagnetic charge and orbital ordered insulating domains. Experiments in this field were performed by means of diverse techniques ([2—17]). At that time, V.G. Bar'yakhtar with co-authors ([18—21]) have developed a theoretical description of the domain structures emerged in antiferromagnets during the first-order magnetic phase transition driven by an external magnetic field. It was also suggested [2, 3, 9, 10] that, in antiferromagnets, there exist inhomogeneous states similar to either the intermediate or mixed states in type I and type II superconductors, respectively, under destroying superconductivity by the external magnetic field. The thermodynamic analysis has shown that the spatial distribution of inhomogeneous states is governed by the sign of interfacial energy, independently of their nature. In fact, the intermediate states were observed in spontaneously magnetized substances, both ferro- and antiferromagnets, in non-ferrous materials under conditions of the de Haas—van Alfven effect [22] and in superconductors ([23] and references therein). The less studied similarities of the mixed state formation in the different types of substances are considered here for the uniaxial crystals of superconducting dichalcogenide 2H-$NbSe_2$ and antiferromagnetic ferrous carbonate $FeCO_3$. Their transverse magnetization components derived from the high-field measurements (Figs. 1,2) are analyzed in a framework of thermodynamic approach.

2. Thermodynamic Analysis of Magnetization

Transverse magnetization investigations proved to be an effective tool for studying a spatially inhomogeneous magnetic state. They revealed the intermediate [2] and mixed [9] states in antiferromagnets alike those in type I and type II superconductors, respectively. To register the transverse magnetization of an anisotropic crystal in a uniform magnetic field, the torque measuring technique is available. It was successfully applied for a long time in the studies of the magnetic anisotropy and the Fermi surface [24]. In the Gaussian units, a torque τ is described by the relation

$$\tau = -M_{\perp} H V, \tag{1}$$

where H is the external magnetic field, V is the sample's volume, $M_{\perp}$ is the transverse (with respect to the applied magnetic field) component of the absolute magnetization, $M_{\perp} = M_x \cos\Theta - M_z \sin\Theta$, z is directed along the c axis, x is the direction along the a or b axis in the ab plane, and Θ is the angle between the c axis and the external magnetic field direction. The observation of torque on the samples suggests a nonzero magnetization component off from the magnetic field direction and, consequently, the orientation dependence of free energy of the sample in a magnetic field. The intrinsic torque in superconductors gained a detailed analysis [28] after the first observation of the turning of fine particles of an anisotropic high-temperature superconductor by a magnetic field [25–27]. Transverse magnetizations of uniaxial superconductor 2H-$NbSe_2$ and easy-axis Ising antiferromagnet $FeCO_3$ is first compared in the present work.

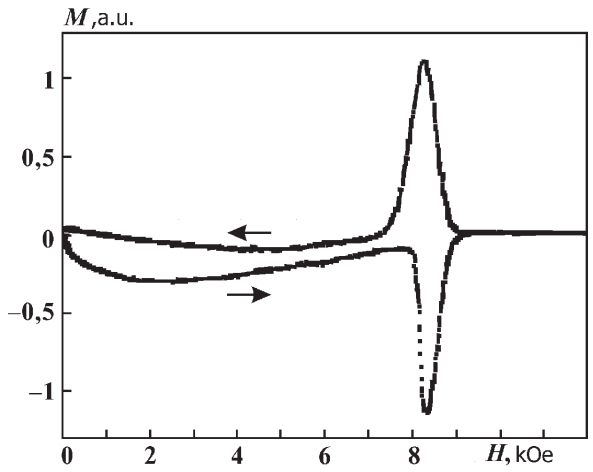

Fig. 1. Magnetization of uniaxial superconductor 2H-$NbSe_2$ vs the external magnetic field

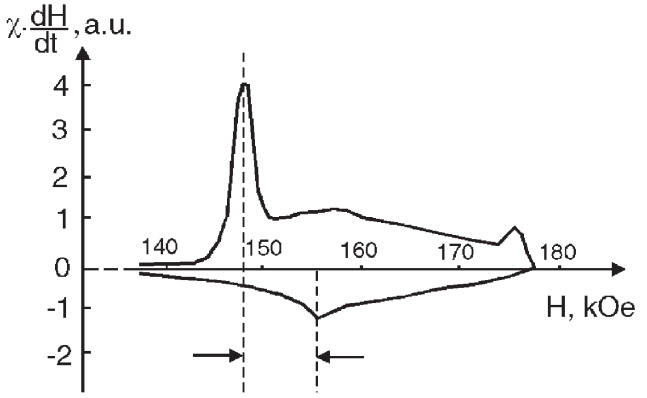

Fig. 2. Magnetization of uniaxial antiferromegnet $FeCO_3$ in a magnetic field pulse of the amplitude $H_{\max} > H_2$. The arrows point out the curve feature shift

2.1. Anisotropic superconductor

In the Gaussian units [29], a superconductor in a magnetic field is described by the thermodynamic equality

$$G_i = F_i(T, B_i) - \frac{B_i H}{4\pi}, \tag{2}$$

where G_i and F_i are the Gibbs potential and free-energy density, respectively, of the i-phase. The mixed state or else, the Shubnikov phase, and the phase with $B \equiv H$, where the major volume fraction retains the normal state, are labeled by indices i and j, respectively. The ratio of the magnetic field and the induction in the mixed state is assigned by the minimum condition for G at definite H and T:

$$\frac{\partial}{\partial B_i} F_i(T, B_i) = \frac{H}{4\pi}. \tag{3}$$

The thermodynamic Gibbs potential for the array of interacting vortices is defined as follows:

$$G = n_L \mathcal{F} + \sum_{i,j} U_{ij} - \frac{BH}{4\pi}, \tag{4}$$

where $\mathcal{F}$ is the free-energy density of an isolated vortex, n_L is the number of vortices in unit volume, U_{ij} is the vortex repulsion potential, and

$$B = n_L \Phi_0. \tag{5}$$

In such a way, the first term in (4) describes the net energy of isolated vortices. The second term in (4) is the vortex repulsion energy. The third term in (4) accounts the external field effect. It tends to favor large values of the induction B. This means that the external field H is the virtually external pressure which tends to increase the vortex density.

The following analysis of the measurements will incorporate quantitative estimate of the vortex interaction in the range $H_{c1} \ll H \ll H_{c2}$, in which the average intervortex distance a_0 obeys the inequality $\xi \ll a_0 \ll \lambda$. The quantity ξ is the superconducting coherence length, $a_0 = \sqrt{\Phi_0/B}$ is the vortex lattice parameter, and λ is the penetration depth ($1/\lambda^2 \ll n_L \ll 1/\xi^2$)). Within such a range of vortex lattice parameters and the field, the free-energy density of a *uniform* superconductor in the London limit ($\lambda \gg \xi$) is [29]

$$F = \frac{B^2}{8\pi} + \frac{B}{4\pi} H_{c1} \frac{\ln(\beta a_0/\xi)}{\ln(\lambda/\xi)}, \tag{6}$$

where β is a constant of the order of unity, which depends upon the flux line lattice structure. It is considered as a parameter to be found from experimental data. Then, the magnetization M is readily found as

$$-4\pi M = (\Phi_0/8\pi\lambda^2) \ln(H_{c2}\beta/H). \tag{7}$$

In fact, the considered field range is restricted from below by the field $H' > H_{c1}$, beyond which the irreversibility can be ignored, so that the relationship (7) holds in a field range

$$H' < H \ll H_{c2}.. \tag{8}$$

The London equations may be generalized to the case of anisotropic superconductor by substituting the isotropic effective mass for the anisotropic mass tensor

[30]. Then eq. (6) transforms to the free-energy equation of the tilted vortex lattice

$$8\pi F = B^2 + (\Phi_0/4\pi\lambda^2)(m_1 B_x^2 + m_3 B_z^2)^{1/2} \ln(H_{c2}\beta/B), \tag{9}$$

where m_1 and m_2 are the in-plane components of the mass tensor; $m_1 = m_2$ in a uniaxial superconductor, and m_3 is that in the c-axis direction. By minimizing (9) with respect to B, the magnetization components are

$$-M_z = M_0 \frac{m_3 \cos\theta}{\sqrt{m(\theta)}}, \quad -M_x = M_0 \frac{m_1 \sin\theta}{\sqrt{m(\theta)}}, \tag{10}$$

where θ is the off c-symmetry axis angle and

$$M_0 = \frac{\Phi_0}{32\pi^2\lambda^2} \ln\frac{H_{c2}\beta}{H}, \quad m(\theta) = m_1 \sin^2\theta + m_3 \cos^2\theta. \tag{11}$$

2.2. Easy-axis antiferromagnet

Let us consider the plane case of a two-sublattice antiferromagnet with uniaxial anisotropy. In a proper theoretical description, the thermodynamic potential [31] or, else, the energy density is commonly represented as

$$\Phi = \frac{A}{2} \cdot \vec{m}^2 + \frac{a}{2} \cdot m_z^2 + \frac{b}{2} \cdot l_z^2 - \vec{m} \cdot \vec{h}, \tag{12}$$

where $\vec{h} = \vec{H} \cdot M_0$, $\vec{m} = (\vec{M}_1 + \vec{M}_2)/M_0$, $\vec{l} = (\vec{M}_1 - \vec{M}_2)/M_0$, $|\vec{M}_1| = |\vec{M}_2| = M_0$, z is the direction along the principal crystallographic axis, $\vec{M}_1$, $\vec{M}_2$ represent magnetic moments of sublattices. Their moduli are assumed constant, which is true for the lowest temperatures $T \ll T_N$, with T_N being the Neel temperature of antiferromagnetic ordering. $\vec{H}$ is the external field; $\vec{m}$, $\vec{l}$ are the vectors of ferro- and antiferromagnetism, respectively.

In expression (12), the first term is referred to the exchange energy, and the second and third terms are the energies of crystal anisotropy.

For antiferromagnets with the "easy axis" anisotropy, which is the case of $FeCO_3$, $b < 0$. Under the additional condition of $(a + b) < 0$, the minimization of Eq. (12) yields the dependence $m_z(h_z)$. It describes the so-called spin-flop transition. The antiferromagnet with the absolute values of anisotropy constants exceeding enough the exchange interaction constant A undergoes a direct transition into the saturated ferromagnetic state in the applied magnetic field h_z, omitting the spin-flop. The first situation was observed by J.S. Jacobs on manganese fluoride MnF_2, the second one was registered by J.S. Jacobs [32], and later on by V.I. Ozhogin [34] on $FeCO_3$.

It is important to note that the first-order character of the spin-flop transition in an external magnetic field adjusted with great precision in the z-direction is lost, when $\vec{h}$ tilts off from the z-axis by an angle ψ beyond the critical value ψ_c. The critical angle is determined by the magnetic anisotropy field and the exchange field ratio corresponding to the ratio $|b|/A$ [35]. For instance, the critical angle of MnF_2 is $\psi_c \approx 30'$ (thirty angular minutes).

3. Experimental Part

Ferrous carbonate $FeCO_3$ is a transparent antiferromagnet with strong uniaxial magnetic anisotropy [32] which has been postulated to be an ideal Ising system [33]. Its magnetic properties arise predominantly from the effect of a cubic crystal field with the trigonal distortion and spin-orbit coupling in the ^5D ground state of a Fe^{2+} ion [33]. The magnetic excitations at low temperatures have been measured by neutron, infrared, and Raman scattering, as well as by Mossbauer studies. To investigate these excitations, the external magnetic field and internal exchange interactions also have been considered. It should be noted that the spin-lattice coupling exceeds the exchange interactions for an order of magnitude. This system is described in detail in [36]. Its theoretical aspects were discussed in [37] and [38].

Similar to experiments [32] and [34], a magnetic field was generated by a pulsed solenoid, and the measurements were performed using the inductance technique. The magnetic measuring technique for examining inhomogeneous magnetic states in the immediate vicinity of the phase transition should satisfy extremely strict requirements, which are motivated and summarized below:

1. The measured properties should not differ much from those at the absolute zero temperature for the sake of comparison with theory so that the condition $T \ll T_N$ is satisfied, providing the samples are cooled by liquid helium ($T = 4.2$ K).
2. In the vicinity of the phase transition, the magnetic properties rapidly change in a variable field. Then its high uniformity is required just as in measurements of the de Haas—van Alfven effect in metals.

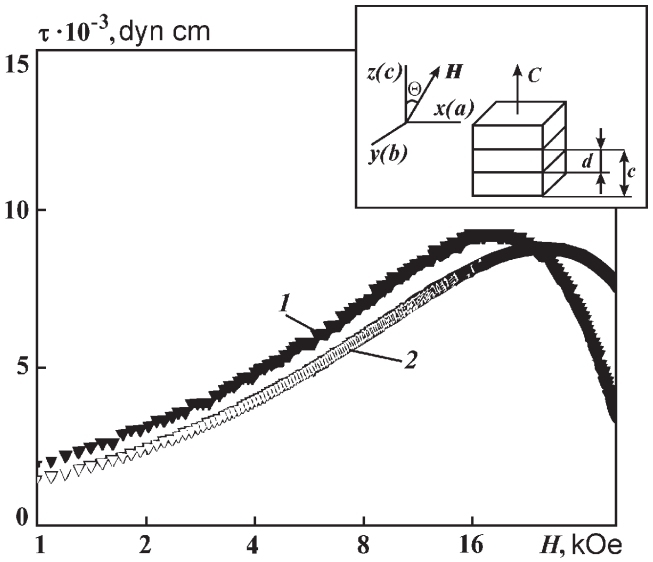

Fig. 3. Semi-log plot of the measured and calculated torque dependences $\tau(H)$ at $T = 4.2$ K. Inset presents the experiment geometry

3. To avoid effects of the relaxation process in the sample, the magnetic field sweep should not be too fast in measurements operating range. So the inductance of a solenoid for the field production was large enough to provide a pulse length of $\approx 15 \times 10^{-3}$ s.
4. Great precision of the magnetic field orientation relative to the crystal axis should be achieved as the permitted error should not exceed one angular minute. To this end, the solenoid was mounted on an isolated plate with the slope varied by means of 4-μm screws.
5. The inductance measuring technique should provide the registration of all three magnetization vector components, which was achieved by winding three coils on a sample.
6. To elucidate carefully the magnetization distribution inside a sample, several pick-up coils were used. They were inductively coupled with different parts of the crystal.
7. To distinguish the narrow region in the intimate vicinity of the phase transition, the threshold scanning circuit was utilized. The oscillographic record started in the field approaching the threshold value H_{thr} just below the critical field H_c. Then the scan scale was magnified by many times.

The observation of the transverse magnetization in the mixed state of a superconductor put the following specific requirements on the samples and experimental techniques employed. 1) The sample should be an anisotropic superconductor. Our sample under study meets this requirement as its anisotropy parameters are close to those of the yttrium high-T_c superconductor, on which the intrinsic torque was first observed. Their effective mass ratios in the c-axis direction and in-plane are 10 and 25, respectively, proving moderate anisotropy. Moreover, due to the uniaxial anisotropy, the superconducting compound 2H-$NbSe_2$ is the most appropriate object for the model description. 2) Pinning effects should be minimal. In fact, the high-quality single crystals of 2H-$NbSe_2$ under study are characterized by the ratio of the depinning and depairing critical currents $j_c/j_o \approx 10^{-6}$ which is low enough to describe them as the cleanest type-II superconductors. Their field dependences of magnetization have two reversible regions, viz., weak fields $H \ll H_{c2}$ and near the upper critical field H_{c2}. 3) As the magnitude of equlibrium magnetization is not large as compared to the applied field (see, e.g., [29]), the torque should be amplified by the sample's volume according to (1). It was realized in our case due to the opportunity of obtaining large crystals of 2H-$NbSe_2$. The volume of the crystal under study was estimated as 19.7×10^{-9} m^3 with accuracy better than 1% on the basis of weight measurements (127 mg) and using the density value 6.44 g/cm^3 calculated from the atomic distribution in the unit cell of 2H-$NbSe_2$ determined from the X-ray measurements. 4) The measurements of total absolute magnetization of 2H-$NbSe_2$ show that the torque signal near the upper critical field H_{c2} should be of the order of 10^{-3} dyn·cm (10^{-10} N·m), if the transverse magnetization were equal to the total magnetization. The available torque measurement technique gave an accuracy of 10^{-5} dyn·cm. This method allowed us to measure the capacitance with an accuracy of 10^{-4}pF. The large-scale magnet M7 at the High Magnetic Field Laboratory in Grenoble provided a highly uniform field in the sample region. The calibration of signals was performed using a miniature coil (diameter 4.8 mm, length 1.4 mm, number of turns 20) mounted in the region of the sample in a field of 12 T with an accuracy of 3%. The out-of-plane angle of the external field direction was estimated as 13° with an accuracy of 1° appropriate for measurements of a torque as a function of magnetic field. The experiment geometry is illustrated by Fig. 3.

The measurements presented in this figure clearly demonstrate the transverse magnetization component of a 2H-$NbSe_2$ single crystal in the field range $H_{c1} \ll H \ll H_{c2}$, with H_{c1} being the lower critical field. It is analyzed below.

4. Discussion

The measured field dependence of the torque is presented by Fig. 3 in comparison with calculations based on the following relation derived on the basis of the London electrodynamics:

$$\tau(H) = \frac{\Phi_0 HV}{64\pi^2\lambda_{ab}^2}\frac{\gamma^2-1}{\gamma^{2/3}}\frac{\sin^2\theta}{\varepsilon(\theta)}\ln\left[\frac{\gamma\eta H_{c2}(\|c)}{H\varepsilon(\theta)}\right]. \qquad (13)$$

Here, Φ_0 is referred to a magnetic flux quantum, ε and γ are the anisotropy parameters,

$$\varepsilon(\theta) = (\sin^2\theta + \gamma^2\cos^2\theta)^{1/2}, \qquad (14)$$

and $\eta \sim 1$.

The compound under study is the classical London superconductor as the penetration depth λ of a weak magnetic field in its interior sufficiently exceeds the coherence length ξ for the M component along the normal to the ab-plane responsible for superconductivity: $\lambda_{ab}\approx$1000 Å and the coherence length $\xi_c\approx$10 Å though larger than the interlayer distance. A satisfactory agreement between the measured and calculated dependences is observed. The region of the apparent deviation of the measured curve from the calculated one is temperature-dependent suggesting a relation of the field $H_{\rm int}$ to the contribution of the intervortex interaction to the magnetization. It is calculated in assumption that the interaction is considerable when the vortex lattice parameter and the penetration depth are identical:

$$a_0 = \sqrt{\frac{\Phi_0}{H_{\rm int}}} = \lambda. \qquad (15)$$

The slope of $M_\perp(\ln H)$ allows one to find the magnetic-field penetration depth λ using Eqs. (10) and (11). The relation derived from the London theory yields

$$\lambda_{ab} = m^*c^2/4\pi n_s e^2, \qquad (16)$$

with $\lambda = 1200$ Å. In a magnetic field as high as 120 kOe, a_0 has the order of the coherence length in the same field direction, i.e. about 20 Å.

5. Magnetic Properties of $FeCO_3$ in the Vicinity of the Antiferromagnet—Ferromagnet Phase Transition

Both the longitudinal and transverse magnetization components were measured. The rate of field sweep ranged within 5—30 $\times$ 10^6 Oe/s. The angle ψ ofthe tilt of $\vec{H}$ from the c_3-axis direction varied within 0—10°. The samples of natural origin were taken from different deposits. Various sample geometries from a cylinder with the axis along [111] direction to a disc with the face normal to [111] direction were examined.

Main results

1. Magnetization in a magnetic field pulse with the amplitude $H_{\rm max}$ of about 180 kOe is shown in Fig. 2. The onset field of the magnetization change is $H_1 = 148$ kOe and the cutoff is $H_2 = 176$ kOe. The susceptibility averaged over the $H_1 \div H_2$ range is 2.7×10^{-2} CGSM.
2. Absolute value of the transverse magnetization component at any angle ψ ($0 < \psi < 10°$) is such that the directions of the total magnetization and the magnetic field $\vec{H}$ coincide suggesting the absence of magnetization components normal to $\vec{H}$ at any values of H and angles ψ.
3. In the vicinity of H_1 and H_2, the sample's magnetization changes faster than that in the intermediate field range $H_1 < H < H_2$. The maximum susceptibility in these regions is almost twice higher than that within the range $H_1 < H < H_2$. The susceptibility amplitude in cylindrical samples with the aspect ratio $\beta = 0.2$ is up to 40% larger than that in disks with $\beta = 5$. The width of the magnetic field interval, $\Delta H = H_1 - H_2$, is practically independent of the sample's shape.

5.1. Magnetic susceptibility in the phenomenological consideration

The trivial phenomenological analysis of the magnetic properties of antiferromagnets commonly deals with the thermodynamic potential including the main interactions related to the spontaneous magnetization of sublattices. The results of such an analysis for moderately anisotropic antiferromagnets [31] are invalid for the description of magnetization measurements on $FeCO_3$ crystals. The pronounced magnetic anisotropy of $FeCO_3$, the absence of the transverse magnetic moment components in experiments with H parallel to c_3 and the published data [39—41] suggest that the thermodynamic potential should include, in this case, the interactions related only to the longitudinal components of the sublattice magnetization vectors. The crystal under study will be first regarded as a two-sublattice antiferromagnet with the sublattice magnetizations denoted as follows:

$$\vec{m}_1 = \frac{\vec{M}_1}{M_0}, \qquad \vec{m}_2 = \frac{\vec{M}_2}{M_0}.$$

Here, M_0 is the spontaneous saturation magnetization identical for both sublattices. The external magnetic

field $h = h_z = H_z/M_0$ is directed along the crystallographic symmetry axis. In this case, the thermodynamic potential of the antiferromagnet is represented as

$$\Phi = -\frac{1}{2}\delta\left(m_1^2 + m_2^2\right) - \gamma m_1 m_2 - (m_1 + m_2)\, h, \qquad (17)$$

with the variables $m_1 = m_{1z}$, $m_2 = m_{2z}$, $m = m_1 + m_2$ changing in the limits

$$-1 \le m_1 \le +1, \quad -1 \le m_2 \le +1, \quad -2 \le m \le +2.$$

Expression (17) is valid for the description of homogeneous states with imperfections not larger than the unit cell dimension. Otherwise the quantities m_1 and m_2 are referred to the sublattice magnetizations averaged over the regions larger than all potential inhomogeneities.

In the absence of a magnetic field, the antiferromagnetic state corresponds to the minimum of (17) with the following relationship between the quantities:

$$\gamma < 0, \qquad |\gamma| > |\delta|$$

or

$$h_1 = -(\gamma - \delta) > 0, \quad h_2 = -(\gamma + \delta) > 0.$$

The minimization of (17) with respect to the variables m_1 and m_2 considering their variation limits yields solutions for the sublattice magnetizations at different magnetic field intensities:

$A)$ $h < h_1$:

$$m_1 = +1,\ m_2 = -1,\ m = 0,\ \Phi_1 = -h_1;$$

$B)$ $h_1 < h < h_2$:

$$\begin{cases} m_1 = +1,\ m_2 = -\dfrac{h+\gamma}{\delta}, \\ m = -\dfrac{h + (\gamma - \delta)}{\delta} \quad (\delta < 0); \\ \Phi_2 = -h_1 - \dfrac{(h - h_1)^2}{h_2 - h_1}; \end{cases}$$

$C)$ $h > h_2$:

$$m_1 = +1,\ m_2 = +1,\ m = +2,\ \Phi_3 = h_2 - 2h.$$

Solution A) which is realized in weak fields corresponds to the antiferromagnetic state. Solution B) describes the high-field ferromagnetic state. The transition from one state into another occurs near the critical field $h_{II} = 1/2\,(h_1 + h_2) = -\gamma$. It is worth noting that only one sublattice changes the magnetization during the transition, while the other maintains the saturation magnetization over the whole range of magnetic field variation. The above-presented equations yield two types of transitions from the antiferro- into ferromagnetic state depending on the sign of the constant δ:

I) If $\delta > 0$, then $h_2 < h_1$ and the reorientation of the second sublattice occurs in field $h = h_2$ by the first-order phase transition. The total magnetization in this field changes jump-likely with $\Delta m = 2$. In the field interval $h_2 < h < h_1$, the metastable states exist and hysteresis is possible.

II) At $\delta < 0$, the field $h_2 > h_1$ and transition occurs continuously in the field interval $\Delta h = h_2 - h_1$. In this interval, solution B) is realized. In an increasing magnetic field, the second-order phase transition occurs at $h = h_1$, and the magnetic susceptibility reveals a jump-like increase $\Delta\chi = \dfrac{2M_0}{H_2 - H_1}$. The linear increase of the magnetization ceases at $h = h_2$, where the second-order phase transition occurs as well, and the magnetic susceptibility vanishes again.

The way of definition of the first term in the thermodynamic potential implies that the constant δ stands for the intrasublattice exchange interaction energy. Its sign is determined predominantly by that of J_{11} which is the sign of the interaction between a singled out ion and those pertained to the second coordination sphere. If the sign of J_{11} favors the ferromagnetic ordering inside a sublattice, the transition under study will be of the first order. Such a situation apparently takes place in layered antiferromagnets $FeCl_2$, $FeBr_2$, etc. [36]. If $\operatorname{sign} J_{11} = \operatorname{sign} J_{12}$, then the transformation occurs continuously with the second-order phase transitions at the onset and at the end.

The comparison of the measured and calculated magnetization curves of $FeCO_3$ shows that the transition in this antiferromagnet tracks type II. Accordingly, the same signs should be ascribed to both the intra- and intersublattice interactions in antiferromagnetic $FeCO_3$. The sign of the intrasublattice interaction in the antiferromagnet may be also found in the molecular field approximation by comparison of the Neel (T_N) and Weiss (Θ) temperatures. The experimental curve allows us to evaluate the ratio of the intra- and intersublattice interaction values:

$$\frac{\delta}{\gamma} = \frac{h_2 - h_1}{h_2 + h_1} = +0.08.$$

We should mention that if the proposed approach describes correctly the magnetization curve of $FeCO_3$,

then the magnetization measurement is the most accurate method to estimate the intrasublattice exchange interaction among all of the known methods. So then, the phenomenological thermodynamic potential (17) incorporating only interactions related to the longitudinal components of sublattice magnetizations provides the sorting of antiferromagnet—ferromagnet transitions, considering the sign of the intrasublattice exchange interaction constant δ. For negative δ, the existence of two critical magnetic fields h_1 and h_2 is described correctly.

5.2. Transverse magnetization components and restrictions of the two-sublattice model

The above-presented phenomenological analysis put no restrictions on magnitudes of transverse magnetization components. Though the thermodynamic potential was chosen in the assumption of their absence, the solutions are formally true in the presence of the transverse magnetization without any contribution to the interaction. That is why a further consideration of their magnitudes is necessary.

The molecular field approximation represents the field and temperature dependences of the sublattice magnetization by the following relations:

$$M_1 = M_0\, B_s(y_1),$$

where $B_s(y_1)$ is the Brillouin function for spin S and $y_i = H_i \mu_B g S/kT$. Therefore, at $T = 0$, a sublattice should saturate ($M_i(0) = M_0$) in any non-zero field. In the magnetic field range $h_1 < h < h_2$, the longitudinal magnetization component of $FeCO_3$ varies continuously. In this situation, if the sublattice magnetization modulus is constant, then the vector $\vec{m}_2$ should turn continuously by an angle of π. A magnitude of the transverse magnetization component should approach M_0 in maximum. However, transverse magnetization components are absent in the experiment. This feature persists under switching on the transverse components of the magnetic field which could align the transverse magnetization components if they were randomly oriented over the crystal. Perhaps, the zero transverse magnetization of sublattices with conservation of the magnetization absolute value in a variable magnetic field might be assumed. However, this idea is in conflict with the results of the two-sublattice model. In such a case, the effective spin $S_{\text{eff}} = 1/2$ should be assigned to an ion, and the interaction of ions should be described in terms of the Ising model. These assumptions are presently confirmed by numerous experiments [39—41]. Consequently, the sublattices of $FeCO_3$ may be only oppositely directed. On the one hand, this is the foundation for thermodynamic potential (17). On the other hand, the bipartition of a sublattice does not explain any intermediate value of its magnetization.

It is reasonable to assume the splitting of the sublattice under study into a large enough number of subsublattices. In the multisublattice approximation, the multistep character of the magnetization curve manifests successive reorientations of subsublattices. The calculated magnetization curve tracks the measured one with any precision as the number of introduced sublattices is practically unlimited.

According to the results of Section 4.2, the physical reason for the sublattice splitting may be regarded as follows. Considering the interaction of sublattices, the minimal energy corresponds to the parallel orientation of their spins. Otherwise, considering the sublattices as isolated subsystems with $\delta < 0$, the minimal energy corresponds to their splitting into several subsublattices with different spin orientations.

The specificity of the current problem is that the external magnetic field h compensates the effective field of the intersublattice interaction $\gamma \cdot m_1$ affecting an isolated sublattice:

$$h_{2\text{eff}} = h + \gamma m_1 + \delta m_2.$$

In such a way, the magnetic field lifts the degeneracy of this sublattice. It splits into n components. Their field is represented by the expression

$$\sum_{j=1}^{n} \gamma_{ij} m_j = \delta + 2\sum_{j=1}^{k} \gamma_{ij} = -\delta - 2\sum_{j=k+1}^{n} \gamma_{ij}.$$

Here, $m_j = M_j/M_{0j}$ is the reduced magnetic moment of the j-th sublattice which can attain the values $m_j = \pm 1$, ($\Delta m_j = \pm 2$) and γ_{ij} are the relevant molecular field coefficients. The total value of this field may range from $-\delta$ in the antiferromagnetic state (all $m_j = -1$) to $+\delta$ in the ferromagnetic one ($m_j = +1$ for all j). he right-hand side of the equality includes the summation only over k or $(n-k)$ sublattices with reversed or unreversed magnetization.

For positive γ_{ij}, the overturn of the j-th sublattice suppresses the effective magnetic field at the sites of the other. This is why their reorientation in the increasing external magnetic field occurs not at once but gradually one by one.

Therefore, the result describing a continuous change of the longitudinal magnetization may be agreed with the experimental finding of the absence of transverse magnetization components, in assumption of the splitting of individual sublattices into a large number of subsublattices with the period much larger than that of the initially chosen unit cell. Thus, the magnetic state of the crystal may be considered as inhomogeneous in the field range $h_1 < h < h_2$. Its periodicity is determined by that of subsublattices and may change in a variable magnetic field.

5.3. Phase transitions and short-range order in the vicinity of the critical fields h_1 and h_2

It is impossible to calculate the total magnetization curve $M(H)$ in terms of the multisublattice model since the molecular field coefficients γ_{ij} are unknown. Nevertheless, it is possible to show that most of them are about zero. Then the part of the magnetization curve in the vicinity of the critical fields h_1 and h_2 can be described together with the corresponding magnetic structures.

The exchange interaction is known to rapidly decay at distances r_0 in a crystal on the scale of several atomic spacings. In the multisublattice model, the sublattice period d is large enough ($d \gg r_0$), and the exchange field at a given point is absent when all ions of the sublattice are far from the point or is produced by a nearest-neighbor ion. In other words, the coefficients γ_{ij} are zero or turn out to be dependent on the spacing r_{ij} between a nearest-neighbor ion belonging to the j-th sublattice and the i-th point. Hence, in the expression for the net field at a site pertained to the i-th sublattice, it is possible to take on summing over ions nearby this site.

Assume that the orientation of ions belonging to the i-th sublattice reverses at such a critical value of the external field h_i that the net effective field at them vanishes:

$$h_i = -(\gamma - \delta) + 2\sum_{j=1}^{k} \gamma_{ij}(r_{ij}).$$

Here, the summing is performed over ions near by the i-th site which have already reversed their orientation. If all γ_{ij} coefficients are positive, the magnetization process starts in the field $h_1 = -(\gamma - \delta)$ with the orientation reversal for the spins at the individual sites spaced a distance r_0 apart.

For $r_0 \to \infty$, the second-order phase transition should occur in the field $h = h_1$ as is stated by the phenomenological analysis. The interaction between the reversed spins gives gain in the total energy if $\gamma_{ij} > 0$, which is virtually their repulsion. Consequently, the energy of ions with reversed spins is minimum when they form a regular close-packed structure[1]. In the increasing magnetic field, the parameter of such a lattice should smoothly decrease.

The crystal magnetization value is available in the estimation of the average spacing between reversed spins. Therefore, the measured $M(H)$ curve allows one, in principle, to find the important dependence $H_{\text{eff}}(r)$ of the effective exchange field on the spacing between interacting spins. The measured magnetization curve (Fig. 2) reveals a sharp decrease near H_1. Such measurements are not secure against the effect of their mean errors on a curve shape. This is why the aforementioned dependence $H_{\text{eff}}(r)$ was not worked out. In estimation of true errors of the curve measurements near H_1, we juxtapose this area with the model of infinite abrupt jump, that is the first-order phase transition. This jump is easy to be justified.

If the interaction radius of reversed spins r_0 is finite, a fair amount of spins reverses in the field H_1. They should be arranged in a regular lattice with the spacing equal to the exchange interaction radius r_0. Here, r_0 has the meaning of a minimal distance, at which the magnetization curve shape remains within the prescribed error, as yet unaffected by this interaction. Using the measured value of the magnetization change in the vicinity of H_1, the fraction of jump-likely reversed spins can be estimated as $\sim 12.5\%$, in agreement with their average spacing in plane (111) $r_0 = 9.4$ Å. To discuss the jump of magnetization observed at H_2, critical field at the site is expressed as:

$$h_i = -(\gamma + \delta) - 2\sum_{j=k+1}^{n} \gamma_{ij}(r_{ij}),$$

where the summing is performed over ions with still unreversed spins. The analysis similar to the above-presented one suggests the presence of a magnetization jump and the occurrence of a magnetic structure near the critical field $h_2 = -(\gamma + \delta)$ similar to that close to the field h_1.

The arrangement of reversed spins in the crystal at $h = h_1$ may be represented by isolated threads aligned

[1] This structure, similar to the mixed state of superconducors, represents a triangular lattice in (111) plane.

with the external magnetic field. They carry a quantum of the additional magnetic flux:

$$\Delta\Phi_0 = 4\pi\mu_B \frac{4S}{d} \approx 0.2 \times 10^{-10}\,\text{Oe}\cdot\text{cm}^2,$$

where μ_B is the Bohr magneton, S is the spin of a Fe^{2+} ion equal to 4/2, and d is the distance between the nearest overturned spins along [111] direction equal to 5×10^{-8} cm. This flux value turns out to be by four orders of magnitude smaller than the magnetic flux quantum in conventional type 2 superconductors.

Thus, the calculated magnitude of the field produced at a site by individual ions together with the distance dependence explain the observed jump-like changes of the magnetization at $h = h_1$ and $h = h_2$. As a result of the first-order phase transition, the reversed spins are arranged in a close-packed structure with the period $r_0 \sim 10^{-7}$ cm.

5.4. Energy of phase boundary and comparison with transition of destroying the type-2 superconductivity by a magnetic field

The examined earlier transition from the antiferromagnetic to ferromagnetic state has much in common with the destroying of superconductivity by a magnetic field. Transitions in superconductors are assorted in consideration of the interfacial energy at the phase boundary dividing the normal and superconducting phases. If the interfacial energy σ is positive (type-1 superconductors) in the infinite medium, the magnetization changes abruptly at $h = h_1$, while the susceptibility is infinite, i.e. the first-order phase transition occurs. If the sign of σ is negative (type-2 superconductor), the transition smoothly starts and terminates in second-order phase transitions. In the infinite medium, the mixed inhomogeneous state emerges in the field range $h_1 < h < h_2$.

The magnetization curves for type-1 and type-2 superconductors are identical with those derived in the phenomenological analysis of type-1 and type-2 transitions from the antiferromagnetic state into the ferromagnetic one. To extend this correspondence, we indicate that the interface energy of the phase boundary dividing the antiferromagnetic and ferromagnetic phases in the above-presented model is positive for the type-1 transition, while it is negative for that of type 2.

It was shown earlier that, apparently, individual spins in $FeCO_3$ align only in opposite directions, the intermediate orientations being forbidden. So we start immediately with the sharp phase boundary of a definite shape, within which a phase transition occurs over the atomic spacing.

Assume for simplicity that each ion interacts with the neighbors belonging to the first and second coordination spheres. In the former, a Fe^{2+} ion in $FeCO_3$ has six nearest neighbors spaced in adjacent layers (111) at a distance of 3.7 Å. J_{12} labels the interaction energy for each pair with parallel spins. The second coordination sphere retains six ions in a plane layer (111) spaced out at a distance of 4.7 Å. J_{11} labels the appropriate interaction energy. Then the interaction energies per one magnetic ion in the antiferromagnetic and ferromagnetic phases and at the phase boundary are, respectively:

$$E_A = +6J_{12} - 6J_{11},$$

$$E_P = -6J_{12} - 6J_{11} - \mu_0 H,$$

$$E_B = -4J_{11} - \frac{\mu_0 H}{2}.$$

In the absence of a magnetic field, the minimal energy of the antiferromagnetic phase with the considered distribution of ions over sublattices corresponds to $J_{12} < 0$ and $|J_{12}| > |J_{11}|$. If $h \gg -\gamma$, the ferromagnetic phase is thermodynamically stable. In the external magnetic field $H_1 = -12J_{12}/\mu_0$, both phases possess equal energies. The extra energy attributed to the phase boundary in the field H_1 is:

$$E_{AP} = E_B - E_A = q2J_{11},$$

where q labels the number of ions per unit area of the boundary. Consequently, the interfacial energy in this model can have any sign regulated by that of the intrasublattice exchange interaction energy.

Hence, the sign of the interface energy unambiguously coupled with the sign of the intrasublattice exchange interaction immediately indicates the type of the antiferromagnet—ferromagnetic transition in an applied field.

The traditional description of antiferromagnets operates in terms of magnetic sublattices. To explain even the magnitude of spikes on the magnetization curve at H_1 and H_2, the amount of sublattices should far exceed two. As is indicated earlier, a periodic inhomogeneous state appears in an antiferromagnet in the critical magnetic field range if its interfacial energy is negative. As in type-2 superconductors, its formation is governed by the decay law of interaction described by the correlation radius. Unlike conventional type-2 superconductors with the correlation radius $\sim 10^{-5}$ cm, that of antiferromagnets equals $\sim 10^{-7}$ cm akin

to uniaxial 2H-$NbSe_2$ superconductor in the utilized experimental configuration.

Thus, the considered magnetization curves of antiferromagnetic $FeCO_3$ and a type-2 uniaxial superconductor have much in common. In both cases, the phase transition in a magnetic field is spread over a finite field range. The onset of transitions is accompanied by the magnetization jump with a spike on the magnetic susceptibility curve. And, finally, magnetization curves possess a noticeable hysteresis. These formal attributes indicate the analogy of transitions in physical objects of different nature. The type of transition is determined by the sign of the interfacial energy at the phase boundary dividing two co-existent states in a crystal.

A certain similarity is also observed in physical processes in the critical magnetic field interval. Let us consider these processes in a plane being normal to the external magnetic field. At first, a transition into the emergent state occurs at isolated points. At the moment of nucleation, they are spaced infinitely apart. A magnetic flux quantum is coupled with each isolated point. Because of the repulsion, they form a regular periodic structure in the plane being perpendicular to field direction. The interaction of the points decays exponentially so that they are rapidly brought closer by the increasing field. This process leads to the infinite slope of the magnetization curve. If the interaction vanishes at $r > r_0$, the magnetization first changes jump-likely. This gives rise to an inhomogeneous structure with period r_0. A further increase of the field is bringing the points closer more smoothly due to their considerable interaction. Then the magnetization curve possesses a finite slope, and the magnetization increases as long as the sample completely transforms to a fresh homogeneous state.

6. Summary

In conclusion, we emphasize that a comparative thermodynamic analysis of the magnetization processes in a uniaxial superconductor and an antiferromagnet over the field range of the phase transition into the normal and ferromagnetic state, respectively, has shown that they share some characteristics. Those are determined for both cases by the minus sign of the interfacial energy of the phase boundary between the co-existent phases. The transitions develop in field intervals extended between the lower and upper fields, at which the onset and the end of a transition are accompanied by jump-like changes of the magnetization. There exist similar spatially inhomogeneous magnetic states described just as the mixed state or else the Shubnikov phase of type-2 superconductor. These results confirm the general law of formation of the intrinsic inhomogeneous magnetic states in the vicinity of phase transitions induced by the external magnetic field in substances of different physical nature, governed by the sign of the interfacial energy on the phase boundary between the co-existent states.

1. *Dagotto E., Takashi Hotta, Moreo A.* // Phys. Repts. — 2001. — **344**, N 1—3. — P. 1—153.
2. *Dudko K.L., Eremenko V.V., Fridman V.M.*// Sov. Phys. JETP. — 1967. — **34**, N 2. — P. 362—367.
3. *Dudko K.L., Eremenko V.V., Fridman V.M.*// Ibid. — 1971. — **61**, N 4. — P. 1553—1563.
4. *Galkin A. A., Kovner S. N., Popov V.A.*// Phys. status solidi (b). — 1973. — **57**. — P. 485—495.
5. *King A.R., Paquette D.* // Phys. Rev. Lett. — 1973. — **30**, N 14. — P.662—666.
6. *Mil'ner A.A., Popkov Yu.A., Eremenko V.V.* // Sov. Phys. JETP Lett. — 1973. — **18**, N 1. — P.20—22.
7. *Mil'ner A.A., Popkov Yu.A., Eremenko V.V.* // Ibid. — P. 39—42.
8. *Bar'yakhtar V.G., Galkin V.A., Telepa V.T.* // Fiz. Nizk. Temp. — 1975. — **1**, N 4. — P. 483—485.
9. *Dudko K.L., Eremenko V.V., Fridman V.M.*// Sov. Phys. JETP. — 1975. — **68**, N 2. — P. 659—671.
10. *Dudko K.L., Eremenko V.V., Fridman V.M.*//Ibid.— N 6. — P. 1157—1160.
11. *Kharchenko N.F., Szymczak H., Eremenko V.V.* // Sov. Phys. JETP Lett. — 1977. — **25**, N 5. — P. 258—262.
12. *Rezende S.M., King A.R., White R.M., Timble J.P.* // Phys. Rev. B. — 1977. — **16**, N 3. — P. 1126—1131.
13. *Gapon N.V., Dudko K.L.* // Sov. Phys. JETP. — 1979. — **77**, N 4(10). — P. 1528—1543.
14. *Eremenko V.V., Klochko A.V., Naumenko V.M.* // Sov. Phys. JETP Lett. 1982. — **35**, N 11. — P. 479—481.
15. *Eremenko V.V., Klochko A.V., Naumenko V.M., Pishko V.V.* // Ibid. — 1984. — **40**, N 6. — P. 219—221.
16. *Eremenko V.V., Klochko A.V., Naumenko V.M., Pishko V.V.* // Fiz. Nizk. Temp. 1985. — **11**, N 3. — P. 327—331.
17. *Eremenko V.V., Klochko A.V., Naumenko V.M.* // Sov. Phys. JETP. — 1985. — **88**, N 9. — P. 1002—1017.
18. *Bar'yakhtar V.G., Borovik A.E., Popov V.A.* // Sov. Phys. JETP Lett. — 1969. — **9**. — P. 634—637.
19. *Bar'yakhtar V.G., Borovik A.E., Popov V.A., Stefanovsky E.L.* // Sov. Phys. JETP. — 1970. — **59**, N 10. — P. 1299—1306.
20. *Bar'yakhtar V.G., Borovik A.E., Popov V.A., Stefanovsky E.L.* // Sov. Phys. Solid State Physics. — 1970. — **12**, N 11. — P. 3289—3297.
21. *Bar'yakhtar V.G., Borovik A.E., Popov V.A.* // Sov. Phys. JETP. — 1972. — **62**, N 3. — P. 2233—2241.

22. *Condon J.H., Walstedt R.E.* // Phys. Rev. Lett. –– 1968. –– **21**, N 9. –– P. 612––614.

23. *Eremenko V.V., Sirenko V.A.* // Magnetic and Magnetoelastic Properties of Antiferromagnets and Superconductors. — Kyiv: Naukova Dumka, 2004 (in Russian).

24. *Shoenberg D.* Magnetic Oscillations in Metals. — Cambridge, 1986.

25. *Tranquada J.M., Goldman A.J., Moodenbaugh A.R.*// Phys. Rev. B.— 1988.— **37**. — P. 519.

26. *Solin S.A., Garsia N., Vieira S., Hortal M.* // Phys. Rev. Lett. — 1988. **60**. — P. 744.

27. *Chechersky V.D., Eremenko V.V., Finkel V.A., Kaner N.E.* // Low Temp. Phys. — 1989. — **15**. — P. 52.

28. *Kogan V.G.* // Phys. Rev. B.— 1988— **38**.— P. 7049.

29. *De Gennes P.G.* Superconductivity of Metals and Alloys.— New York: Benjamin, 1970.

30. *Kogan V.G.* // Phys. Rev. B. — 1981. **24**. — 1572.

31. *Turov E.A.* Physical Properties of Magnetically Ordered Crystals.— (Moscow: Academy of Sciences of USSR, 1963 (in Russian).

32. *Jacobs J.S.* // J. Appl. Phys. — 1963. — **34**. — P. 1106—1107.

33. *Kanamori J.* // Prog. Theor. Phys. — 1958. — **20**.— P. 890.

34. *Ozhogin V.I.* // Zh. Eksp. Teor. Fiz. — 1963.— **45**. — P. 1687—1693.

35. *Kaganov M.I., Chepurnikh G.K.* // Solid State Phys. — 1969. **11**. — P. 911—917.

36. *Borovik-Romanov A.S., Grimmer H.*//International Tables for Crystallography. — Volume D: Physical Properties of Crystals./ Ed. by A. Authier. — Dordrecht: Kluwer, 2003. — P. 105—149.

37. *Zhou Yi-Yang , Yin Chun-Hao* // Phys. Rev. B. — 1993. — **47**, N 9. — P. 5451—5454.

38. *Ivanov M.A., Loktev V.M., Pogorelov Yu.G.* // Fiz. Nizk. Temp. — 1985. — **11**, N 6. — P. 620—630.

39. *Alikhanov R.A.* // Zh. Eksp. Teor. Fiz. 1959. — **36**. — P. 1690—1696.

40. *Forester D.W., Koon N.C.* // J. Appl. Phys. — 1969. — **40**. — P. 1316.

41. *Hang Nam Ok* // Phys. Rev. — 1969. — **185**. — P. 472—476.

ХАРАКТЕРНІ НЕОДНОРІДНОСТІ В АНТИФЕРОМАГНЕТИКАХ ТА НАДПРОВІДНИКАХ

В.В. Єременко, В.А. Сіренко

Р е з ю м е

Досліджено спільні риси формування неоднорідних магнітних станів в одновісних антиферомагнетиках та надпровідниках поблизу фазових перетворень, що індукуються зовнішнім магнітним полем. Обговорюється поперечне намагнічування кристалів надпровідної сполуки дихалькогеніду ніобію 2H-$NbSe_2$ та антиферомагнітного сидериту $FeCO_3$. Використовуючи термодинамічний підхід, доведено, що головні характеристики фазового перетворення та неоднорідні магнітні структури, що формуються протягом перетворення, зумовлені знаком енергії межі поділу співіснуючих фаз не залежно від фізичної природи неоднорідних станів.

ХАРАКТЕРНЫЕ НЕОДНОРОДНОСТИ В АНТИФЕРРОМАГНЕТИКАХ И СВЕРХПРОВОДНИКАХ

В. В. Еременко, В.А. Сиренко

Р е з ю м е

Исследованы общие черты формирования неоднородных магнитных состояний в одноосных антиферромагнетиках и сверхпроводниках вблизи фазовых преобразований, которые индуцируются внешним магнитным полем. Обсуждается поперечное намагничивание кристаллов сверхпроводящего соединения дихалькогенида ниобия 2H-$NbSe_2$ и антиферромагнитного сидерита $FeCO_3$. Используя термодинамический подход, доказано, что основные характеристики фазового преобразования и неоднородные магнитные структуры, которые формируются в процессе преобразования, обусловлены знаком энергии границы раздела сосуществующих фаз не зависимо от физической природы неоднородных состояний.